

For

$$E_{\max} = 6 \text{ GeV}$$

$$N \approx 1.9 \left( \frac{2^{3/2} K m c^2}{V_N} \right)^{\frac{1}{2}}.$$

We choose

$$V_N = 100 \text{ kV}, K = 5, N \approx 714 \text{ frequencies.}$$

The minimum frequency spacing is given by

$$\frac{\omega_0}{\omega_2} = K \left( \frac{V_N}{2^{3/2} K E_2} \right)^{\frac{1}{2}} = 6.0 \times 10^{-3} \text{ at 6 GeV}$$

$\omega_2$  is about 1 Mc at 6 GeV, then the basic repetition rate is 6 kc.

The different frequencies would be applied to drift tube electrodes located at radial positions where the frequencies are effective. This would eliminate difficulties due to different harmonic orders of the same frequency. With thirty electrodes located along one circumference, a peak voltage of 100 kV would produce about 100 kV peak acceleration per turn. Then there would be about 23 accelerating electrodes located on one radius.

## DISCUSSION

DZHELEPOV: What would be the number of frequencies in each and what number of electrodes should you have with a machine for 600 MeV?

ROBINSON: I have been describing a 300 MeV machine. Are you asking about another machine now from the ones I described? For a 600 MeV machine of what type? Of an FFAG type or of a cyclotron type? For a cyclotron type, if we obtained something like 6 or 7 MeV per electrode, we would then require the order of a hundred frequencies.

MARTIN: My question is with respect to the fixed frequency cyclotron. I did not understand how the electrodes are arranged.

ROBINSON: It would be a drift-tubes type structure as is used in a cyclotron at present, except it would be divided in

such a way that there are divisions between separate electrodes such that the lower frequencies would be applied to the electrodes to the outside and the higher to the inside.

MARTIN: I should also like to ask if you made any calculations concerning the radial amplitudes developed in the beam using an acceleration scheme of this sort?

ROBINSON: No, not really. One will have to be somewhat concerned with phenomena similar to RF knock-out. You would have to avoid exciting radial betatron oscillations by a frequency which was non-synchronous.

It seems that when the total frequency change is small, all this is not much of a problem.

## AIR-CORE STRONG FOCUSING SYNCHROTRON

**N. C. Christofilos**

Lawrence Radiation Laboratory, University of California, Livermore, Cal.

### I. INTRODUCTION

There are two distinct directions to be considered in the planning of future high-energy accelerators: high energy, much higher than the accelerators presently under construction (CERN, Switzerland; Brookhaven National Laboratory, USA), namely of the order of 100 BeV; or moderate energy, 10 to 30 BeV, but much higher current of the order of a few micro-amperes.

Steel magnets have certain inherent limitations. In the case of very high energy, the circumference of a steel magnet becomes undesirably large. The only way to reduce the length of the circumference is to use higher values of magnetic field (i.e., 50 000 G) which are possible only with air-core magnets. The air-core magnets are allegedly associated with high stored energy. However, with proper coil design

(\*) This work was performed under the auspices of the U.S. Atomic Energy Commission.

it is possible to reduce the stored energy to the same value as in a steel-magnet machine for the same particle energy. This can be obtained by reducing the size of the magnet, and by proper arrangement of the current distribution in the coils. The peak power requirements of such a magnet are rather high. However, this can be considerably reduced by operating the magnet at a temperature of 80° K or lower. Recent developments in cryogenics, or rather the necessity of building large refrigeration units for other applications, resulted in a considerable reduction of the cost of such units. Hence, application of cryogenics in accelerators is now under consideration, although positive conclusions are not yet possible. In addition to the reduction of the required peak power it is possible to reduce considerably the average power by contemplating a short acceleration time, less than one-tenth of a second. This shorter acceleration time requires in turn a more powerful RF amplifier but this is necessary anyway, if it is desired to accelerate a large number of particles per pulse, to compensate for azimuthal space charge forces in the bunch. An additional advantage of the high field value is that the particle density in the bunch becomes high enough so that synchroclash operation might be possible without the necessity of storage rings.

## II. MAGNET COILS

The magnet coils are confined between two coaxial cylinders of radius  $r_i$  and  $r_o$  respectively (Fig. 1). The cylinder of radius  $r_i$  is the vacuum chamber. Thus the aperture of the machine is of circular cross-section. The required field in the aperture is a dipole field (the guiding field) combined with a quadrupole focusing field. The solution of the vector potential within the coil must satisfy the boundary conditions;

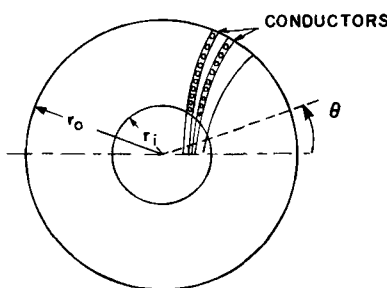


Fig. 1 Schematic of cross-section of coil.

namely, to match the field components of the vacuum field in the aperture and in the space outside the coil. The current distribution ( $j$ ) within the coil is then determined from the equation

$$\frac{4\pi j}{10} = -\nabla \times (\nabla \times A_z), \quad (1)$$

where  $z$  is along the axis of the coil.

There is a variety of functions which can satisfy these conditions. However, the calculations are much simplified by employing Bessel functions as solutions for the vector potential within the coil. Hence, the solutions can be identical with solutions of Maxwell equations for time-varying fields where the displacement current has been substituted by the actual current distribution in the coil. These solutions for each harmonic (of  $n$ th order) assume the form

$$A_z = -\frac{B_0}{k} C_n(kr) \cdot \cos(n\theta), \quad (2)$$

where

$$C_n(kr) = c_1 J_n(kr) + c_2 Y_n(kr)$$

and  $J_n$ ,  $Y_n$  are the Bessel functions of  $n$ th order of the first and second kind, respectively.

The boundary conditions are (see Appendix I)

$$C_{n+1}(kr_i) = 0$$

$$C_{n-1}(kr_o) = 0.$$

By integrating the square of the field and the current density we can determine the stored energy and the power loss respectively, as a function of the ratio  $r_o/r_i$  of the outer to the inner radius of the coil. A plot of these two quantities as a function of  $r_o/r_i$  is shown in Fig. 2. The stored energy varies almost linearly with  $r_o/r_i$  while the power loss increases rapidly for values of  $r_o/r_i$  less than 2. In the example cited hereafter a ratio of  $r_o/r_i \approx 3$  has been selected. For this particular example, the current density distribution  $j$ , the power loss  $W_R$ , and the stored energy  $W_0$  are given by the following equations:

$$j = \frac{2 B_0}{\pi r_i} [C_1(k_1 r) \cos \theta + 1.5775 \alpha C_2(k_2 r) \cos 2\theta] \text{ A/cm}^2, \quad (3)$$

where

$$C_1(k_1 r) = 2.3711 J_1(k_1 r) + 0.076221 Y_1(k_1 r)$$

$$C_2(k_2 r) = 3.9448 J_2(k_2 r) + 0.04738 Y_2(k_2 r)$$

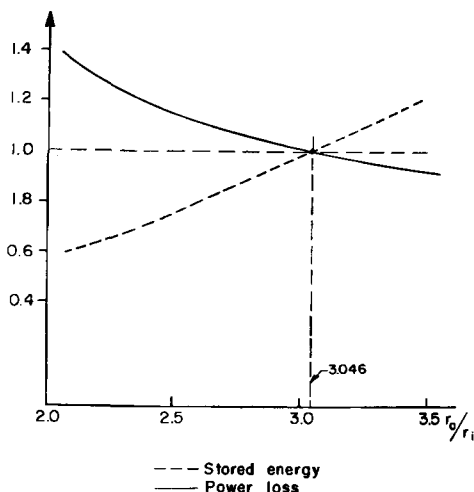


Fig. 2 Variation of the stored energy and power-loss with the ratio of the outer to the inner coil radii.

$J_1$  and  $J_2$  are Bessel functions of the first kind of the first and second order, respectively.

$Y_1$  and  $Y_2$  are Bessel functions of the second kind of the first and second order, respectively.

$$k_1 r_i = 0.8$$

$$k_2 = 1.5775 k_1$$

$B_0$  = peak value of the field at the orbit (G)

$r_i$  = the inner radius of the coil in cm

$a$  = the ratio of the quadrupole to the dipole field strength at  $r = r_i$ .

$a = 0.3375$  in the following examples.

The power loss in the coil is

$$W_r = (\rho/\eta) B_0^2 k_i^2 r_i^2 \left\{ (r_0^2/r_i^2) C_1^2(k_1 r_0) - C_1^2(k_1 r_i) + (k_2 \alpha/k_1)^2 [(r_0^2/r_i^2) C_2^2(k_2 r_0) - C_2^2(k_2 r_i)] \right\} W/cm, \quad (4)$$

and the total stored energy on the magnet is

$$W_0 = 5r_i^2 (B_0^2/8.10^8) \left\{ (r_0^2/r_i^2) C_1^2(k_1 r_0) - k_1^2 r_i^2 + \alpha^2 [(r_0^2/r_i^2) C_2^2(k_2 r_0) - (k_2^2 r_i^2/4)] \right\} J/cm, \quad (5)$$

where  $\rho$  is the resistivity ( $\rho = 1.72 \times 10^{-6}$  for copper at  $300^\circ$  K) and  $\eta$  is the space factor; in the following examples it is assumed that  $\eta = 0.58$ .

More details on the calculations of the magnet are included in Appendix I.

### III. MAGNET UNITS, RF CAVITIES

The magnet units consist of a pair of magnet coils enclosed in a cylindrical evacuated tank (Fig. 3). This tank serves also as a radio-frequency cavity where each coil is approximately a quarter wavelength at the highest frequency. The gap between the two coils serves as an accelerating gap. In this way, straight sections for pump connections and acceleration are not necessary, thus enabling a smaller circumference length. The tuning of the cavity can be done with rotating condensers up to 1% of the frequency. The fine tuning ( $\pm 1\%$ ) can be accomplished with ferrite coils disposed in series with the rotating condensers. Thus the effect of the low  $Q$  of the ferrite is minimized and an overall  $Q$  of 1500 is expected for each cavity. Furthermore, by having a plurality of accelerating cavities we minimize the overall RF power requirements. Since the required volts per turn is rather high, in order to keep the amplitude of the phase oscillations within reasonable limits a high harmonic RF order of 30 or more, is required.

The dimensions of the magnet coils and the cavity in an example are :

Aperture	2.5 cm
Outer coil diameter	8 cm
Cavity diameter	60 cm
Cavity length	100 cm
Field index $\left[ n = \left( \frac{\partial B}{\partial R} \right) \frac{R}{B} \right]$	450
Betatron oscillations per turn, "v"	8

The acceleration time is assumed as 0.06 seconds. The power source of the magnet can be either motor-generators or a condenser bank. It appears that for such a short acceleration time the cost of a capacitor bank is comparable with the cost of motor-generator units. However, detailed cost estimates are not yet available at this time. In my opinion, though, other conditions being equal, condenser banks are preferable to motor-generators with all their rotating equipment.

In the calculation of the power losses a 60 millisecond linear rise of the magnetic field has been assumed. At the peak value a "flat top" of 10 milliseconds has been included. A decay time of 60 milliseconds has been postulated. Continuous operation

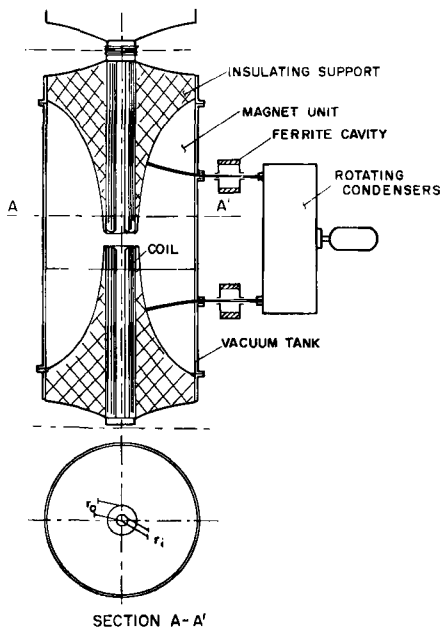


Fig. 3 Schematic of the cross-section of the machine.

of the machine at 60 cps is also possible. In this case, the magnet current varies as

$$I = I_0(1 + \cos \omega t). \quad (6)$$

This is accomplished by d.c. biasing of the magnet. The a.c. is provided by a capacitor bank. The power loss in this case is rather high. Hence, a.c. operation must be considered only in a case where very high current is required. It should be noted that a machine built initially for pulsed operation can be converted later to continuous a.c. operation if higher current is required.

#### IV. PARTICLE INJECTION, SPACE CHARGE LIMIT

The number of particles per pulse which can be trapped are limited by the allowed change of the number of betatron oscillations " $v$ " due to the space charge forces in the bunch. We have assumed an (allowable)  $\delta v = 0.25$  in calculating the number of particles per unit length of the machine. Since the number of trapped particles increases with the injection energy, a higher than usual injection energy can be employed, inasmuch as the linear accelerator cost is not a large part of the overall cost of the machine. For one-turn injection the linear accelerator current becomes too high. Hence, multturn injection

appears more attractive. The most promising way for multturn injection, in my opinion, is the molecular injection, namely, to accelerate  $H_2^+$  and split the molecules upon injection with a mercury jet or otherwise. Of course in this way the particles must be accelerated up to twice the injection energy. However, no other way of multturn injection appears to me at this time as promising as the molecular injection.

An injection energy of 80 MeV has been postulated. This in turn requires that the  $H_2^+$  ions must be accelerated up to 160 MeV. The resulting number of accelerated particles per pulse (for  $\delta v = 0.25$ ) is  $6 \times 10^{12}$ . In order to maintain all these particles as they go through the phase transition, it is desirable to avoid any blow-up of the beam at the phase transition. Consequently, a mode of variation of the accelerating voltage was sought which would allow finite amplitude of the phase and momentum oscillations near the transition energy. This investigation was fruitful and it turned out that in a rather simple way one can find solutions for the phase oscillations, thus avoiding the blow-up problem. The required variation of the accelerating voltage  $V$  near the phase transition is given by the equation

$$(V \cos \phi_s) - V_s = - \frac{\tau}{T_s} V_i \cos \phi_0, \quad (7)$$

where  $\phi_s$  is the instantaneous value of the equilibrium phase;  $V_s$  is the effect of the space charge of the bunch (which actually at the phase transition energy is negligible);  $\tau = t - t_0$ ;  $t_0$  is the time the transition occurs; and  $T_s$  is a constant. The resulting solution of the phase oscillation is (see Appendix II)

$$\phi = C_0 \cos (\alpha \tau^2 + \delta). \quad (8)$$

At the transition point the bunch is exactly at the crest of the wave ( $\phi_s = \pi/2$ ), and the accelerating voltage is equal to the threshold voltage per turn. Beyond the phase transition, the accelerating voltage is gradually increased up to the initial value and the equilibrium phase is restored to the original value but at the other side of the wave. By employing this method it appears that the amplitude of the phase oscillations at the end of the acceleration becomes a small fraction of the betatron oscillations. Since this method is not particular to the proposed accelerator, it can be tried on any of the accelerators now under construction.

## V. ACCELERATOR PARAMETERS

As an illustrative example, the parameters for a 24 BeV accelerator are listed below.

Particle energy (BeV)	24
Orbit radius (m)	16
Aperture (cm)	2.5
Peak value of the magnetic field at the orbit (G)	51 000
Field index "n"	450
Approximate "v" value	8
Number of magnet units	96
Stored energy in the magnet (MJ)	3.8
Duration of acceleration (ms)	60
Peak R F volts per turn	$6 \times 10^6$
Harmonic order (frequency range 32-80 mc)	32
Injection energy (MeV)	80
Number of particles accelerated per pulse	$6 \times 10^{12}$
Final beam cross-section (cm <sup>2</sup> )	0.1
Final beam current density (A/cm <sup>2</sup> )	150
Magnet operating temperature (°K)	80
Magnet time constant (ms)	62
Peak magnet power (MW)	240
Average magnet power (15 pulses/min) (kW)	1 500
Cryogenics plant power (approx.) (kW)	10 000

In comparison, for operation at room temperature, the peak value of the magnetic field must be restricted to 25 kG. Then all the dimensions of the machine become twice as large, namely  $R = 32$  m, and the aperture 5 cm. The stored energy is also doubled. The required peak power is 500-700 MW while the average power is 4000-6000 kW depending on the coil space factor. If the additional cost for the larger motor generator capacity is higher than the cost of the cryogenics plant (in the above example), then the first set of parameters is preferable inasmuch as the beam current density is 4 times as high as in the second case.

A detailed cost estimate of the machine is not available at this time. However, preliminary estimates indicate that it is not much in excess of a conventional A.G.S. machine.

We shall discuss here in more detail the derivation of the relations for the calculations of the parameters of the coils. As mentioned in Section II, the aperture of the magnet is a cylinder of radius  $r_i$  and the con-

ductors are located between two cylinders of radius  $r_0$  and  $r_i$ , respectively. The field components are in the  $r, \theta$  (Fig. 1) direction only. The current direction is along the  $z$ -axis, which is parallel to the

For example, one could at first build a 24 BeV machine for pulsed operation. Later, after this machine is completed, there are two choices :

- (a) to provide the necessary equipment for 60 cps operation, thereby having a very high current machine; or
- (b) to build an additional 100 BeV machine and operate both at synchroclash, thereby obtaining 100 BeV at the c.m.s.

Since today it is not clear which of the two solutions is preferable, it is very desirable to build a machine which potentially can be extended later either towards high current or towards very high energy at the centre of mass system.

## APPENDIX I

ductors are located between two cylinders of radius  $r_0$  and  $r_i$ , respectively. The field components are in the  $r, \theta$  (Fig. 1) direction only. The current direction is along the  $z$ -axis, which is parallel to the

axis of the cylinders ( $r_0, r_i$ ). The vector potential in the current-free regions can be written for any field with  $2n$  poles as follows :

region  $0 < r < r_i$  :

$$A_z = B_0 r_i (r^n/nr_i^n) \cos(n\theta); \quad (9)$$

region  $r > r_0$  :

$$A_z = -c_0 B_0 r_0 (r_0^n/nr^n) \cos(n\theta), \quad (10)$$

where  $c_0$  is a dimensionless constant.

Within the coil region we have

$$\nabla \times (\nabla \times A) = -4\pi j/10, \quad (11)$$

where  $j$  is the current density in the coil.

By assuming that

$$4\pi j/10 = k^2 A_z, \quad (12)$$

the solution of  $A_z$  is given in Bessel functions of the first and second kind, thus :

$$A_z = -(B_0/k)[c_1 J_n(kr) + c_2 Y_n(kr)] \cos(n\theta) \quad (13)$$

or

$$A_z = -(B_0/k)C_n(kr) \cos(n\theta). \quad (13a)$$

The boundary conditions are that the field components are matched at the boundaries and the resulting relations are

at  $r = r_i$  :

$$C'_n(kr_i) = 1, \quad (14)$$

$$nC_n(kr_i)/kr_i = 1; \quad (14a)$$

at  $r = r_0$  :

$$C'_n(kr_0) = -c_0, \quad (15)$$

$$nC_n(kr_0)/kr_0 = c_0. \quad (15a)$$

From Eqs. (14) — (15a) and the recurrence formulas, we obtain

$$C'_n(kr_i) - [nC_n(kr_i)/kr_i] = -C_{n+1}(kr_i) = 0 \quad (16)$$

$$C'_n(kr_0) + [nC_n(kr_0)/kr_0] = C_{n-1}(kr_0) = 0. \quad (17)$$

The requirements of Eqs. (16) and (17) result in that

$$J_{n-1}(kr_0)/Y_{n-1}(kr_0) = J_{n+1}(kr_i)/Y_{n+1}(kr_i). \quad (18)$$

$k$  is determined from Eq. (18) and  $c_0, c_1, c_2$  from Eqs. (14)-(16). Finally by substitution in Eq. (12) the current distribution is specified. By constructing the coil with the thus-specified current distribution the desired field can be realized. By assuming the

solutions in Bessel functions one has the convenience of existing tabulations, recurrence formulas, etc.

The stored energy in all three regions is obtained from the integral

$$W_0 = (10^{-7}/8\pi) \int_{0,0}^{\infty,2\pi} B^2 r dr d\theta \text{ J/cm} \quad (19)$$

and the losses from the integral

$$W_{r0} = (\rho/\eta)(10/4\pi)^2 k^4 \int_{r_i,0}^{r_0,2\pi} A_z^2 r dr d\theta \text{ W/cm.} \quad (20)$$

The actual losses depend on the time variation of the field; in the case where the current varies as  $(1+\cos\omega t)$ , the actual losses are

$$W_r = (3/8)W_{r0}. \quad (21)$$

Any combination of harmonics can be obtained by adding linearly the corresponding vector potentials.

Analogous solutions can be obtained in axial symmetric field configuration in spherical co-ordinates; in the spherical case the coil is assumed to be confined between concentric spheres of radius  $r_i$  and  $r_0$ ; then for a  $2n$ -pole field the solution of the vector potential in the coil region is assumed thus :

$$A_\phi = (B_0/k\sqrt{kr})C_{n+1/2}(kr) \quad (22)$$

with the condition that

$$C_{n+3/2}(kr_i) = 0 \quad (23)$$

$$C_{n-1/2}(kr_0) = 0. \quad (23a)$$

The other constants are determined by the same procedure as in the cylindrical case.

In the cylindrical case we observe from Eqs. (20) and (21) that the power loss is independent of the scaling factor, whereas the stored energy is proportional to the square of the radius  $r_i$ .

The actual coil construction presents some practical difficulties. Since many conductors must be connected in parallel, it is required that the emf is the same in each group of parallel conductors; otherwise the current distribution will be disturbed. The emf is in the  $z$ -direction; namely,

$$E_z = -\frac{1}{c} \dot{A}_z. \quad (24)$$

We observe that according to Eq. (24) the emf is constant along surfaces of constant vector potential. This in turn means that the emf is constant on surfaces

whose trace on a plane  $z = \text{constant}$  are magnetic lines. Hence groups of conductors connected in parallel must be placed on such surfaces. If  $N$  is the (total) number of conductor groups desired to be connected in series, we shall divide the coil area in  $N$  zones where in each zone

$$\int jr dr d\theta = I_0/N, \quad (25)$$

where  $I_0$  is the total current in the coil (in the case where all the conductors were connected in parallel). After the zones have been determined, the conductors are placed in the center of each zone.

## APPENDIX II

The well-known equation for the phase oscillations is

$$\frac{d}{dt} \left( \frac{\gamma}{\Gamma} \frac{d\phi}{dt} \right) + \omega_0^2 \frac{hV_i \cos \phi_0}{2\pi V_0} \phi = 0, \quad (26)$$

where  $\Gamma = \left( \frac{1}{\gamma^2} - \frac{1}{v^2} \right)$  (26a)

$\gamma = E/M_0 c^2$  (the relativistic mass ratio)

$v$  = the number of betatron oscillations per turn  
 $\omega_0 = c/R$  the Larmor frequency of a particle with velocity  $c$

$h$  = the harmonic order

$V_0 = M_0 c^2/e$

$\phi$  = the phase angle in respect to the equilibrium phase

$\phi_0$  = the equilibrium phase

$V_i$  = the applied RF voltage per turn.

The phase transition occurs when

$$\gamma \equiv \gamma_0 = v. \quad (27)$$

The adiabatic approximate solution of Eq. (26) is

$$\phi = \text{const} (\Gamma/\gamma)^{\frac{1}{2}} \cos (\int \Omega dt + \delta), \quad (28)$$

where

$$\Omega = \left( \frac{V_i \cos \phi_0 \Gamma}{2\pi V_0 \gamma} \right)^{\frac{1}{2}}. \quad (28a)$$

Near the phase transition the approximation is not valid and it is customary to assume that  $\Gamma$  is varying linearly with time. Then the solutions admitted are Bessel and Neumann functions of order  $2/3$ <sup>1)</sup>. In the present case this solution was not considered satisfactory and a new one was sought in order to avoid beam blow-up during the phase transition. I assumed that near the phase transition the equilibrium phase is shifted with time according to the equation

$$(V \cos \phi_s) - V_s = -\frac{\tau}{T_s} (V_i \cos \phi_0), \quad (29)$$

where  $V_s$  results from the space charge of the bunch (this quantity is however negligible at the phase transition and it can be deleted from the equation);  $\phi_s$ ,  $V$  are the instantaneous values of the equilibrium phase and applied accelerating voltage, respectively;  $\tau = t - t_0$ ;  $t_0$  is the time the transition occurs, and  $T_s$  is a constant with dimensions of time. This quantity must be larger than the transition mistiming due to momentum spread.

We assume that the quantity  $\Gamma$  varies linearly with time :

$$\Gamma = \frac{1}{\gamma^2} - \frac{1}{v^2} = -(\tau/\gamma_0^2 T_0), \quad (30)$$

where

$$T_0 = (\gamma^3/2\dot{\gamma}\gamma_0^2) \approx (\gamma_0/2\dot{\gamma}) \quad (31)$$

and

$$\dot{\gamma} = \dot{E}/M_0 c^2. \quad (32)$$

Upon substitution in Eq. (26) we obtain

$$\ddot{\phi} - \frac{\dot{\phi}}{\tau} + \omega_1^2 \left( \frac{\tau^2}{T_0 T_s} \right) \phi = 0, \quad (33)$$

where

$$\omega_1 = \omega_0 (hV_i \cos \phi_0 / 2\pi V_0 \gamma_0^3)^{\frac{1}{2}}. \quad (34)$$

Equation (33) admits the solution

$$\phi = \frac{\tau}{T_s} [c_1 J_{\frac{1}{2}}(\alpha \tau^2) + c_2 Y_{\frac{1}{2}}(\alpha \tau^2)], \quad (35)$$

where

$$\alpha = \frac{\omega_1}{2T_s^{\frac{1}{2}} T_0^{\frac{1}{2}}}. \quad (35a)$$

Substituting the Bessel and Neumann functions by their trigonometric expressions we obtain

$$\phi = c_1 \cos (\alpha \tau^2) + c_2 \sin (\alpha \tau^2) \quad (36)$$

or

$$\phi = c_0 \cos (\alpha \tau^2 + \delta). \quad (37)$$

We observe that Eq. (37) is the desired solution. As long as the equilibrium phase varies as prescribed

by Eq. (27), the amplitude of the phase oscillations remains constant; thus blow-up of either phase or momentum oscillations is avoided.

Equation (31) indicates that  $\dot{\gamma}$  must remain constant during the time the phase shifts. Consequently the applied voltage times the sine of the equilibrium phase must remain constant during the same time interval; namely,

$$V \sin \phi_s = V_i \sin \phi_0. \quad (38)$$

Equations (29) and (38) yield

$$\cot \phi_s = \tau / T'_s \quad (39)$$

$$\sin \phi_s = \left[ \frac{1}{1 + \left( \frac{\tau}{T'_s} \right)^2} \right]^{\frac{1}{2}} \quad (40)$$

$$V = (V_i \sin \phi_0) \sqrt{1 + \left( \frac{\tau}{T'_s} \right)^2}. \quad (41)$$

where  $T'_s = T_s \tan \phi_0$ . At  $t = t_0$ , at the phase transition point, the equilibrium phase is  $\pi/2$ , the applied voltage becomes equal to the threshold voltage per turn and the bunch rides at the crest of the accelerating wave.

The amplitude of the momentum oscillations and the corresponding radial oscillations are

$$\frac{\delta p}{p} = c_0 \left[ \frac{(V_i \cos \phi_0) T_0 \gamma_0}{(2\pi h V_0 T_s)} \right]^{\frac{1}{2}} \quad (42)$$

$$\frac{\delta R}{R} = \left( \frac{\delta p}{p} \right) / \gamma_0^2. \quad (43)$$

The constants  $c_0$ ,  $\delta_0$  are determined from Eq. (28) at  $\tau = -T_s$ , i.e., at the time where the applied voltage starts to vary in accordance with Eq. (41). Due to the momentum spread all of the particles are not going through the phase transition simultaneously. Consequently, due to this mistiming error as well as non-linear effects, both the amplitude of the phase and momentum oscillations are expected to be somewhat higher than indicated from the above calculations.

#### Acknowledgments

The author is indebted to Drs. Lloyd Smith and David Judd, Lawrence Radiation Laboratory, University of California, Berkeley, and Dr. Keith Symon, Midwestern Universities Research Association, for fruitful discussions during the preparation of this study.

#### LIST OF REFERENCES

1. Courant, E. D. and Snyder, H. S. Theory of the alternating-gradient synchrotron. *Ann. Phys. New York*, 3, p. 40, 1958.

#### DISCUSSION

O'NEILL: I have three questions. 1) Why is it easier to remove heat at  $80^\circ K$  than at a higher temperature? 2) There is a good reason for not trying to carry out the synchroclash operation by building two of these machines, that is, they are already fairly complicated and if you want to do synchroclash you have to put an ultra-high vacuum system in the same machine, which seems like an unnecessary complication. 3) I agree indeed that you could get a higher current density because you are using a smaller radius for the machine but about the same  $Q$ -value as for a big AGS. However, it is hard to see how you get more than about a factor of 100, because the field which is used is certainly no more than ten times the average field in an AGS machine and you would expect that the current density would scale as at most the square of the focusing strength, for a given injection system.

From the viewpoint of the experimenter, straight sections should be very long; magnets are a necessary evil. Since your machine has a betatron wavelength only 1/10 as long as that of a big AGS, the straight section length allowable would also be 1/10 as long or about 1 meter.

CHRISTOFILOS: 1) It is easier to remove the heat simply because you have quite less heat to remove. 2) It would be uneconomical if one had to build two identical machines, but if having a machine which is, say, 100 BeV you build only an additional 25 BeV which constitutes 25% of the cost, then I think this will be cheaper than a storage ring at 100 BeV. That is one thing. The other is that as I am not optimistic about vacuum and I assume a pressure of  $10^{-8}$  to  $10^{-9}$  which appears feasible because the magnets are at very low temperature. Then there is a lot of background, but I assume that the bubble chambers are somewhat removed from the machine and shielded so the background will remain small. 3) The current density is measured at the centre of each bunch, so it is not the average current along the ring as the bunches are five times smaller. The average current is 30 A per  $\text{cm}^2$  but at the centre of the bunch it is about 150 because the bunches occupy only one-fifth of the circumference. In the first case the cross-section of the beam at the end is about one-tenth of a  $\text{cm}^2$ .

WIDEROE: The relative high temperature of  $80^\circ K$  seems to indicate that you are using coils of copper or aluminium and

the calculations show that you then can gain by a factor of 3, or something like that, against 300°K; but the calculations of Post seem to show that if you use coils made out of sodium and go down to a much lower temperature, then you can make a gain up to 25 and this, of course, would be very important just in this case.

CHRISTOFILOS: Well, sodium gives always very much more gain, but only if we consider d.c. magnets. If you consider pulsed magnets, because the conductivity is very high at 10°K, the skin depth is so small that it is completely impractical to use sodium, considering that sodium is a dangerous material and has to be contained inside tubes, and those tubes would be of the order of 1 mm for that case. Therefore the most one can do with that type of pulsed machine is to go to 30°K with aluminium coils.

SANDS: I do not understand how you propose to use these machines for synchroclash, because if I understand they are

pulsed machines and they will remain at the peak energy only a small fraction of the time.

CHRISTOFILOS: Yes, they remain at peak energy a small fraction of the time, but the utility of the machine depends on what type of experiment we do; for example, a bubble chamber operates only for 1 msec. There only are 10 msec in which the experiments can be done; more power is required to extend this time.

SANDS: I think from the point of view of the physicists a synchroclash machine which has a short duty cycle will be a big disadvantage.

CHRISTOFILOS: If the final operation of the machine is at 60 cps, it is possible, with the use of third harmonic, to obtain a flat top, and thus a 15% duty cycle. Moreover, after the synchroclash stage, the particles may be decelerated, thus avoiding all the radiation effects created by the high energy particles.

## SCANNING FIELD ALTERNATE GRADIENT ACCELERATORS

T. Kitagaki (\*) and J. Riedel

Princeton-Pennsylvania Accelerator, Princeton University, Princeton, N. J.

(presented by T. Kitagaki)

Historically, the scanning field alternate gradient accelerator has developed from an idea for a d.c. field synchrotron first conceived in 1953. The essential feature of the scanning field alternate gradient accelerator (SFAG) is to use a scaling d.c. guide field with a gradient, and a scanning quadrupole field giving the opposite gradient for the AG focusing. Because the scanning field need only provide a gradient in the vicinity of the instantaneous orbit, the magnetic energy in this time varying field is quite small compared with the energy of the d.c. guide field.

One type of SFAG accelerator can be called the superposed type SFAG. This is a ring machine similar to the radial sector FFAG, but with positive curvature of orbit everywhere. Alternate sectors

have simple d.c. scaling fields, and the other half have running quadrupole fields superposed on the d.c. scaling guide fields (Fig. 1). The null point of the quadrupole field appears along an instantaneous

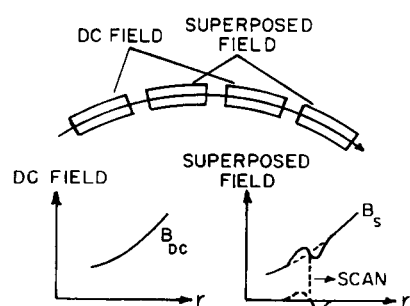


Fig. 1 Superposed type SFAG.

(\*) On leave from Tohoku University, Sendai, Japan